Dalton Transactions

Accepted Manuscript

This is an *Accepted Manuscript*, which has been through the Royal Society of Chemistry peer review process and has been accepted for publication.

Accepted Manuscripts are published online shortly after acceptance, before technical editing, formatting and proof reading. Using this free service, authors can make their results available to the community, in citable form, before we publish the edited article. We will replace this *Accepted Manuscript* with the edited and formatted *Advance Article* as soon as it is available.

You can find more information about *Accepted Manuscripts* in the Information for Authors.

Please note that technical editing may introduce minor changes to the text and/or graphics, which may alter content. The journal's standard Terms & Conditions and the Ethical guidelines still apply. In no event shall the Royal Society of Chemistry be held responsible for any errors or omissions in this *Accepted Manuscript* or any consequences arising from the use of any information it contains.

ROYAL SOCIETY OF CHEMISTRY

www.rsc.org/dalton

ARTICLE TYPE www. rsc.org/xxxxxx | XXXXXXXX

Charge Transfer Processes: the Role of Optimized Molecular Orbitals

Benjamin Meyer,[a] Alex Domingo,*[a] Tim Krah,[a] and Vincent Robert,*[a]

Received Xth XXXXXXXXXX 20XX, Accepted Xth XXXXXXXXX 20XX
First published on the web Xth XXXXXXXXXX 200X
DOI: 10.1039/b000000x

The influence of the molecular orbitals on charge transfer (CT) reactions is analyzed through wave function-based calculations. Characteristic CT processes in the organic radical 2,5-di-tert-butyl-6-oxophenalenoxyl linked with tetrathiafulvalene and the inorganic crystalline material $LaMnO_3$ show that changes in the inner-shells must be explicitly taken into account. Such electronic reorganization can lead to a reduction of the CT vertical transition energy up to 66%. A state-specific approach accessible through an adapted CASSCF (Complete Active Space Self-Consistent Field) methodology is capable of reaching good agreement with the experimental spectroscopy of CT processes. A partitioning of the relaxation energy in terms of valence- and inner-shells is offered and sheds light on their relative importance. This work paves the way to the intimate description of redox reactions using quantum chemistry methods.

1 Introduction

Charge transfer (CT) reactions consist in the displacement of an electron from one chemical region to another. Such process is governed by the laws of thermodynamics, but can also be triggered by some external stimulus. The transfer causes a change of the oxidation states of both reaction partners. Two mechanisms are traditionally reported for CT reactions. The inner-sphere CT reactions are characterized by two redox centres that are chemically connected either by a permanent covalent linkage (intra-molecular CT) or a transitory one (inter-molecular CT). On the other hand, the outer-sphere CT reactions involve redox centres that are not connected by any bridge. In that case, a through-space hopping mechanism occurs between the donor and acceptor sites.

Numerous biological processes such as photosynthesis and respiration involve several CT reactions.[1] Porphyrin-based metal complexes act as cofactors of proteins (*i.e.* haem compounds in haemoglobin) which perform such charge transfer. Despite a rather low efficiency, the electron transport chain allows plants to convert sunlight into chemical energy.[2] More generally, the flow of electron takes part in the production of energy that can be used to fuel the organisms activities.

Such interest in CT reactions is not restricted to fundamental research in biochemistry. With the current growing demand for energy production, CT reactions are an intense field of research in photovoltaics.[3] Porphyrin-based compounds are seriously considered for molecular electronics, being incorporated in dye-sensitized solar cells[4] which can exhibit spectacular conversion efficiencies.[5] Nevertheless, much efforts are also dedicated to purely organic devices.[6,7] Taking advantage of the chemical flexibility of organic compounds, it becomes possible to tune the electronic affinity and ionization energy of the donor and acceptor almost at will. However, the charge separation (so-called photo-induced exciton) is a critical step which calls for fundamental inspection. Recently, the organic radical 2,5-di-tert-butyl-6-oxophenalenoxyl (6OP) has been linked with a tetrathiafulvalene (TTF) moiety (**1**, see Fig. 1).[8] The resulting electron donor (TTF) – acceptor (6OP) system has been considered for solar energy conversion.

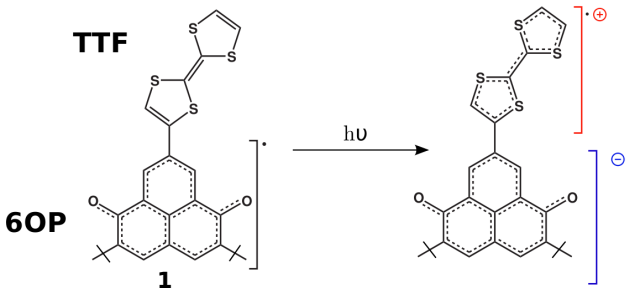

Fig. 1 Structure of the electron donor (TTF) and the electron acceptor (6OP) moeities of **1**.

CT reactions are likely to give rise to unusual magnetic properties in extended systems. In doped $LaMnO_3$ materials, it is widely accepted that ferromagnetic properties result

† Electronic Supplementary Information (ESI) available: [details of any supplementary information available should be included here]. See DOI: 10.1039/b000000x/

[a] *1 rue Blaise Pascal, 67008 Strasbourg, France. Fax: 03 6885 1589; Tel: 03 6885 1302; E-mail: domingo@unistra.fr, vrobert@unistra.fr*

Dalton Transactions Accepted Manuscript

from the double exchange mechanism as originally proposed by Zener.[9] The discovery in the 1990s of colossal magnetoresistance (CMR) at room temperature in manganese oxides[10] renewed the interest in this family of materials.[11] The CMR involves an interrelated change in the ordering of charge, magnetism and crystal lattice degrees of freedom within these perovskite-type manganites. Such phenomena are mainly determined by cooperative effects that arise from a highly correlated character.

The prototype perovskite $LaMnO_3$ (**2**) has a lattice structure formed by corner sharing MnO_6 Jahn-Teller (JT) distorted octahedra, with La ions enclosed in boxes formed by eight MnO_6 groups. Figure 2 shows a schematic representation of the crystalline structure of $LaMnO_3$.[12] The lattice exhibits an alternating orientation in the ab–plane of the long Mn–O bond of the MnO_6 pseudo-octahedra, the so-called collective JT mode. Additionally, the adjacent MnO_6 groups are tilted in the ab directions, leading to O–Mn–O angle values smaller than 180°. The manganese metal ions are formally $3d^4$ Mn^{3+} with a high spin (HS) ground state electronic configuration ($t_{2g}^3 e_g^1$).

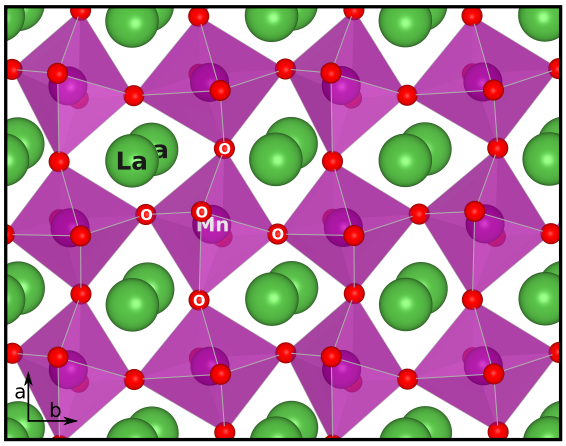

Fig. 2 Lattice structure on the ab–plane of the prototype perovskite $LaMnO_3$.

It is not straightforward to establish the origin of these cooperative effects, which involve the interplay of the electronic structure, the crystal phonons and the lattice structure. Therefore, a microscopic description of the electronic structure of $LaMnO_3$ that is capable to reproduce CT processes and ultimately, the magnetic field-sensitive conductivity would be particularly instructive for this kind of materials.

Regardless of the nature of the phenomenon, intra- or inter-molecular, and the extension of the underlying network, molecular or extended, the description of CT reactions using first-principle calculations is particularly challenging.[13] The inherent charge reorganization that occurs between the ground and charge transfer states must be treated properly, rendering the use of state-average molecular orbitals (MOs) questionable. Thus, there is much interest in developing efficient quantum chemistry methods that can treat synthetic systems combining spectroscopic accuracy, microscopic information of the charge redistribution and an affordable computational cost. Commonly, charge transfer excitations in organic donor-acceptor systems have been computationally characterized within the time-dependent Density Functional Theory (DFT) framework and using many-body Green's function techniques.[14–17] Nevertheless, the standard formalisms based on DFT may not be adapted to describe the electron-trapped character of CT states.[18] The constrained DFT (C-DFT) method was specifically developed to mend this shortcoming of DFT by including an arbitrary constraint to the electronic density.[19–21] Unfortunately, based on our own experience, C-DFT results depend significantly on the choice of the constraint employed.

In the present work, we apply a recently reported strategy based on wave functions calculations to accurately follow CT reactions.[22] By allowing the inactive MOs to adapt, the ground and charge transfer states can be treated on the same footing, leaving out the state-average (SA) strategy to favour a democratic one. This procedure results in an optimal description of the respective electronic distributions present in the context of CT reactions. The methodology is applied to describe the charge transfer between the two moieties of the organic radical-based TTF–6OP (**1**) and the inter-site d–d transition between two adjacent Mn atoms on the ab–plane of $LaMnO_3$ (**2**), the so-called metal-to-metal charge transfer (MMCT).

2 Computational Details

The environment effects present in the ionic crystal **2** were treated within the embedded cluster framework.[26] More precisely, we built a cluster $[Mn_2O_{11}]^{16-}$ to describe the MMCT between two neighbouring MnO_6 sites, which is depicted in Fig. 3. This cluster was embedded in a first layer of *ab initio* model-potentials (AIMP)[27] to reproduce the short-range interactions between the cluster and its closest environment. The AIMPs reduce the electronic dispersion from the cluster to the surrounding cations and, additionally, can incorporate orthogonalization basis functions. In the present case, 12 La^{3+} and 10 Mn^{3+} AIMPs surround the $[Mn_2O_{11}]^{16-}$ cluster. The cluster and the AIMPs are embedded in a distribution of point charges placed on lattice positions. The charge values are optimized to accurately reproduce the Madelung potential on the cluster region.[28] The embedding is formed by 1113 point charges. Similar models to the hereby presented have been successfully employed to study the electronic structure of $LaMnO_3$[29–32] and the same strategy has proven to be ade-

Dalton Transactions Accepted Manuscript

This journal is © The Royal Society of Chemistry [year]

quate to examine localized electronic processes that take place in strongly correlated materials, typical of many transition-metal compounds.[33,34] Even though the $[Mn_2O_{11}]^{16-}$ cluster has no symmetry due to the collective JT mode, we will use the labels of the O_h symmetry group to identify the molecular orbitals of **2**.

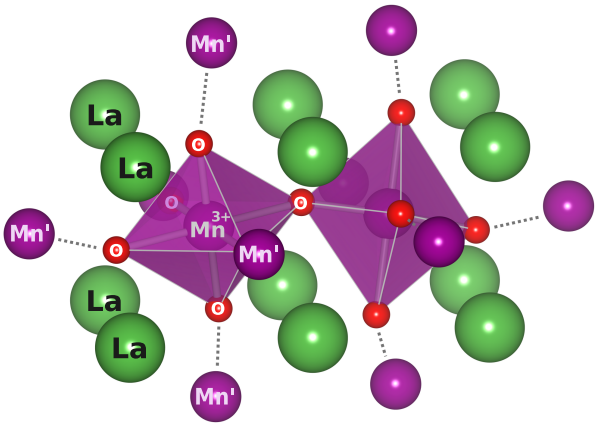

Fig. 3 Structure of the employed cluster model $[Mn_2O_{11}]^{16-}$ with 12 La^{3+} and 10 Mn^{3+} AIMPs. The purple octahedra represent the quantum described cluster region and the surrounding spheres represent model potentials of La (green) and Mn' (purple).

The synthetic organic radical **1** was simplified by changing the tertiobutyl groups into methyl groups to reduce the computational cost. In the subsequent calculations, we checked that this simplification leads to relative energy changes smaller than 8%. All the electronic structure calculations were performed within the MOLCAS 7.6 package.[35] The sizes of the ANO-RCC type atomic basis sets[36,37] used for the electronic structure calculations of **1** and **2** are given in Table 1. Only the contracted basis sets, omitting some polarization functions, were used in the calculations. As reported in the literature,[38] an appropriate representation of the charge distribution relies more on a balanced dressing of the atoms rather than on a systematic use of extended atomic orbital basis sets.

The main objective of this work is to stress the importance of the MOs set in the evaluation of the CT excitation energy. Within the state-average (SA) approach, each state is described based on a common set of MOs. In contrast, state-specific calculations treat each state individually, using a set of MOs fully-adapted to their individual electronic distribution. We explore the effects on the vertical excitation energies induced by the adaptation of the MOs. Thus, we stay in the Born-Oppenheimer approximation and in all cases, we use the ground state geometry of each compound with fixed nuclear positions. Starting from the SA approach in the complete active space self-consistent field (CASSCF)[39] or the restricted active space self-consistent field (RASSCF)[40] calculations, we intend to reach gradually the state-specific description.

Table 1 Basis sets scheme used for **1** and **2**. All orbital angular momenta not shown in the contracted column with respect to the decontracted column were omitted.

Element	Decontracted	Contracted
6OP–TTF (**1**)		
H	$8s4p3d1f$	$1s$
C	$14s9p4d3f2g$	$3s2p1d$
O	$14s9p4d3f2g$	$3s2p1d$
S	$17s12p5d4f2g$	$4s3p1d$
$LaMnO_3$ (**2**)		
O	$14s9p4d3f2g$	$4s3p2d$
Mn	$21s15p10d6f$	$6s5p4d2f$
Mn'	AIMP+$22s16p$	AIMP+$1s1p$
La	AIMP	AIMP

AIMP: Ab Initio Model Potential

The CASSCF wave function is built upon all the possible electronic configurations that span the so-called complete active space (CAS). A minimal CAS was chosen for **1** to account solely for the CT between the TTF and 6OP, namely a CAS[3,2] with 3 electrons in 2 π-like MOs (see Fig. 4). The RASSCF wave function is built upon three active sub-spaces (RAS). This division allows us to limit the total number of excitations incorporated in the wave function. Additionally, as we will see below, this approach facilitates the way to a state-specific description. In the case of **2**, we included in the RAS1 6 electrons in 6 $3d(t_{2g})$-like MOs of the two Mn centres forcing 6 holes to be always present; the RAS2 is formed by 2 electrons in 2 $3d(e_g)$-like MOs, one for each Mn; and the RAS3 included the 2 remaining empty $3d(e_g)$-like MOs of both Mn forcing 0 or 2 particles on them (see Fig. 4). In both cases, the active spaces are constructed to minimize the number of possible electronic configurations incorporated in the wave function. Hence, the CT states appear as low-lying excited states, avoiding the inclusion of other excited states of different nature (*i.e.* intra-metallic d-d transitions, ligand-to-metal charge transfers or intra-ligand π–π^* excitations) that reduce the weight of the CT state in the MOs optimization procedure.

Determining state-specific energies of excited states remains challenging as there is no systematic way to perform such calculations. We devised a procedure that uses the SA result as the starting MOs input and gradually increases the weight of the CT state in the orbital optimization step. The goal is to produce CT state-adapted MOs. The procedure is inspired from recent studies on metal-to-metal charge transfer analysis.[22] At each step, the weight of the CT state is in-

Dalton Transactions Accepted Manuscript

creased to some arbitrary degree and one macro-iteration of the CASSCF is executed. Subsequently, the characters of the resulting states are identified and, if necessary, the distribution of weights is readjusted. Since each state is described with its own set of MOs, we performed a last step consisting in a State Interaction calculation to ensure the orthogonality.[41] On top of the CASSCF and RASSCF, a second-order perturbation theory treatment (CASPT2 or RASPT2)[42] was performed with the default IPEA value of 0.25 hartree and an imaginary shift factor of 0.20 hartree to minimize the intruder state problem.[43]

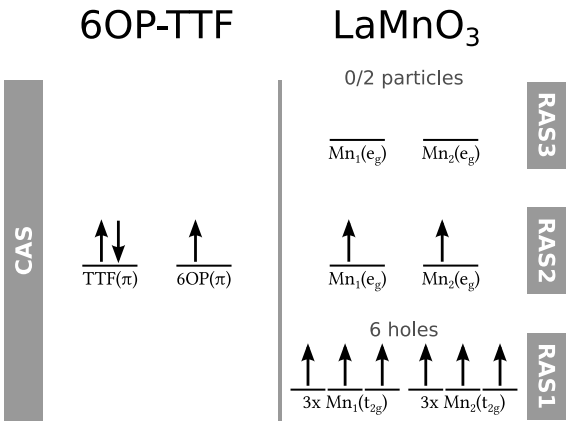

Fig. 4 Definitions of the Complete Active Space used for **1** and the Restricted Active Space used for **2**.

the state-specific ground state energy, calculated within its own set of MOs, is used as a reference. However, the variation lies in the MOs set used for the description of the CT state. It includes an increasing weight of the CT state ranging from 0% (ground state MOs set used for the CT state) to 90% (two distinct quasi state-specific MOs sets for the ground and CT state). Due to convergence problems, we did not manage to go beyond the critical CT weight of 90%. However, the CT energy is reduced by less than 0.05 eV when the CT weight is increased from 80% to 90%. Thus, one can assume that any further modification of the MOs would lead to a negligible change in the vertical energy.

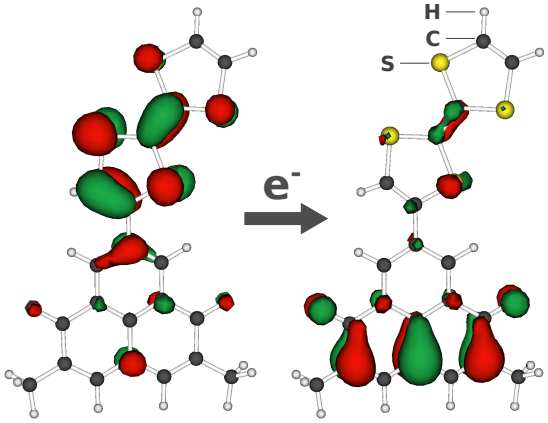

Fig. 5 Molecular orbitals involved in the CT of **1**. The CT occurs between the MOs mainly localized on the TTF (left) and the 6OP moiety (right).

3 Results and Discussion

Having a transferability goal in mind, different CT processes were considered for systems **1** and **2**. The charge excitation of the radical-based organic compound **1** is examined following the aforementioned strategy and its energy is compared to the reported experimental value $\lambda = 1315$ nm (*i.e.* 0.94 eV).[23] Subsequently, the metal-to-metal charge transfer of **2** is estimated following the same procedure. The MMCT of $LaMnO_3$ is reported to be behind the optical absorption band at *ca.* 2 eV for this material.[44–47]

3.1 6OP–TTF

Figure 5 shows the CAS[3,2]SCF active MOs of **1** and stresses its donor and acceptor part. The traditional SA strategy using one set of MOs which is a compromise between the ground and excited states leads to a CT excitation energy of *ca.* 2.13 eV.

The calculated CT excitation energies represented in Figure 6 were obtained in a different manner. All along the curve, Starting from the ground state MOs, the CT excitation energy is 5.08 eV. Evidently, these MOs are fully adapted to describe the ground state and do not offer a good description of the CT phenomenon. Thus, the active MOs were first optimized by freezing all the inactive orbitals and fixing the CT weight to 90%. This first step towards a state-specific point serves to evaluate what we define as the valence-only electronic relaxation energy (see Fig. 6). The latter was estimated to be 0.63 eV, a rather large contribution which cannot be neglected. By allowing the simultaneous inner-shell and valence MOs relaxation, the energy difference drops by 2.85 eV (full electronic relaxation in Fig. 6), a reflection of the sensitivity of the spectroscopy to the MOs definition. If one assumes a strict additivity of both contributions, the inner-shell relaxation energy accounts for 2.22 eV.

These observations are to be contrasted with the CASPT2 values. Indeed, whatever the set of MOs (state-average or state-specific, as previously defined) the CASPT2 CT excitation energy was found to be 1.20 eV, in good agreement with the experimental value. In summary, the gas-phase calculations clearly demonstrate the important role of optimized MOs

Dalton Transactions Accepted Manuscript

This journal is © The Royal Society of Chemistry [year]

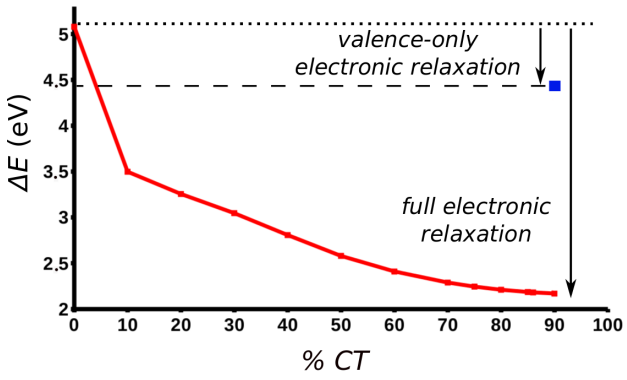

Fig. 6 CT excitation energy ΔE (eV) of **1** with respect to the CT weight. The ground state energy is the CAS[3,2]SCF value.

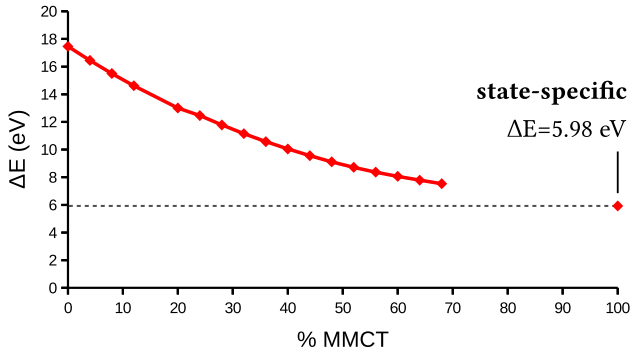

Fig. 7 MMCT excitation energy ΔE (eV) of **2** at the RASSCF level as a function of the MMCT weight on the orbital optimization procedure. The state-specific value is obtained by not allowing any particle in the RAS3.

in the calculation of spectroscopic processes.

3.2 Lanthanum Manganite

The state of affairs might change in molecular architectures where the valence orbitals have a stronger atomic character. Thus, we applied the same strategy to the embedded cluster $[Mn_2O_{11}]^{16-}$ to study the MMCT of **2**. This CT consists in the transition from the HS ground state Mn^{3+}/Mn^{3+}, with two dominant electronic configurations of the form $Mn(t_{2g}^3e_g^1)/Mn(t_{2g}^3e_g^1)$, to the HS excited MMCT state Mn^{2+}/Mn^{4+}, with a dominant electronic configuration $Mn(t_{2g}^3e_g^2)/Mn(t_{2g}^3e_g^0)$. Hence, the MMCT transfers an electron between two 3d(e_g)-like MOs localized on each Mn centre. We computed the lowest five HS states ($S = 8/2$) allowing up to double excitations between the 3d(e_g) MOs on Mn (*i.e.* two particles in RAS3, see Fig. 4). Therefore, the ground state, three intra Mn d–d transitions and the MMCT were simultaneously treated in these calculations. Fig. 7 shows the energy difference ΔE as a function of the MMCT weight on the orbital optimization procedure at the RASSCF level. All along the curve, ΔE is calculated using the state-specific ground state energy (0% MMCT). At this point, the MOs are fully adapted to the ground state charge distribution and hence, we obtain the upper bound limit of the transition (17.46 eV) at this level of theory. Furthermore, as it is observed for **1**, the transition energy is also very sensitive to the MOs definition. Increasing the MMCT weight to 20% and hence, reaching the SA point, recovers *ca.* 25% of the transition energy (13.00 eV). In the present case, it is possible to push the weight up to 68%. Beyond that value, the MMCT state becomes almost degenerate with intra-metallic d–d transitions, mixing with them and hindering the identification of the resulting states. Nonetheless, at 68%, the estimate of the MMCT energy is 7.53 eV, representing a 57% improvement upon the SA solution.

Even though we were not able to increase the MMCT weight beyond 68% due to the presence of other quasi degenerate electronic states, it is still possible to reduce the active space to eliminate any other state than the one of interest. This reduction can be achieved by not allowing any particle in the RAS3 sub-space. Along this scheme, a monoconfigurational description is reached. In practice, we can describe both states by exchanging the corresponding MOs between the RAS2 and RAS3 sub-spaces. Fig. 4 illustrates the setting for the ground state and, for example, the exchange of the $Mn_1(e_g)$ MO of RAS2 with the $Mn_2(e_g)$ MO of RAS3 produces the MMCT state. Obviously, this approach kills the purpose of multiconfigurational methods like RASSCF, but it is necessary in order to improve the description of one particular excited state such as the MMCT of **2**. Since a significant part of electronic correlation is missing at the CASSCF or RASSCF level, there is always a trade-off between the number of effects included in the calculation (*i.e.* the size of the active space) and the quality of the result obtained for a specific excited state. The larger the active space, the more versatility of the wave function, but also more electronic states become accessible and ultimately, the set of orbitals is less adapted to one particular state.

Applying this technique to **2** results in two separate calculations that have a different arrangement of the active orbitals. One describes the HS ground state, with an electronic configuration of the form $Mn(t_{2g}^3e_g^1)/Mn(t_{2g}^3e_g^1)$, and the other describes the MMCT state, with an electronic configuration $Mn(t_{2g}^3e_g^2)/Mn(t_{2g}^3e_g^0)$. The energy difference between these two states with their adapted set of MOs is 5.98 eV, which fits well with the extrapolation of the curve in Fig. 7. Additionally, the state-specific MMCT value is much closer to the reported 2 eV value than the SA result obtained from using the same SA

Dalton Transactions Accepted Manuscript

orbitals for both ground and MMCT states, which results in a transition energy of 12.51 eV. Surprisingly, this very large relaxation of the MMCT does not translate in any relevant modification of the shape of the orbitals involved in the transition. Fig. 8 shows the MO losing one electron in the ground state and the MO accepting one extra electron in the MMCT state. They are clearly 3d(e_g)-like orbitals very well localized on the Mn centres and these characteristics are not altered once the state-specific level is reached. On the other hand, one of the holes in the 3d(t_{2g})-like MOs of Mn, becomes partially delocalized over a 2p MO localized on a first-neighbour O ligand. Thus, the adaptation of the orbitals involve a reduction of the formal MMCT character of the CT state by *not* constraining the induced hole in the metal centre.

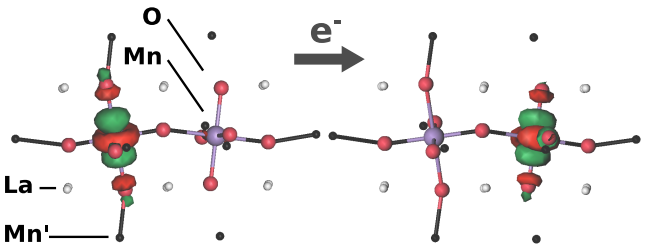

Fig. 8 Molecular orbitals involved in the MMCT of **2**. Left: MO losing one electron in the ground state. Right: MO gaining one electron in the MMCT state.

In spite of having achieved a significant improvement for the estimate of the MMCT transition, the value of 5.98 eV stays still far from the 2 eV value reported in the literature. The state-specific RASSCF result is based on a mono-configurational description that does not incorporate any amount of electronic correlation effects. By means of a second-order perturbation treatment performed over the ground and MMCT states, we capture a larger amount of electronic correlation. The absolute energies of those states at the RASPT2 level are lowered by 91.6 and 90.9 eV, respectively. These large contributions do not improve the MMCT excitation energy though, with a value that reaches 6.70 eV. Nevertheless, the MMCT energy at the RASPT2 level is very stable and does not depend significantly on the imaginary shift parameter (0.1 eV variation between 0.2–1.0 hartree of shift), which is an improvement over previous studies that reflects the better quality of the state-specific reference.[48]

4 Conclusion

The CT processes in the organic radical 6OP–TTF (**1**, Fig. 1) and the inorganic crystalline material $LaMnO_3$ (**2**, Fig. 2) were examined based on wave function calculations. By devising a strategy that allows the evaluation of the energy of both states involved in the CT process on the same footing, not only an improved construction of MOs sets is delivered but a detailed analysis of the electronic structure relaxation energy is offered. The adaptation of the MOs to the CT state of **1** recovers 66% of the transition energy, resulting in a value of 2.22 eV (Fig. 6). This result offers a good reference to perform a subsequent CASPT2 step to include more electronic correlation effects that leads to a value of 1.20 eV, in good agreement with the experimental result (0.94 eV). In the case of the MMCT of **2**, the adaptation of the MOs also recovers 66% of the transition energy, resulting in a value of 5.98 eV (Fig. 7). However, the mono-configurational wave function needed to reach the state-specific value is too limited to treat enough electronic correlation effects, which are very important in **2**, and our estimate stays far from the reported value (2 eV). Along this framework, one can also separately access the valence- and inner-shell reorganization contributions (Fig. 6). Besides, the evaluation of the correlation energy is improved by accounting for the mean-field modifications resulting from charge transfer and the stability of a subsequent perturbative treatment is significantly improved. This work can be considered as a step towards the construction of spectroscopy that incorporate the leading electronic phenomena in the orbitals optimization.

Acknowledgements

This work was supported by the excellence network Chemistry of Complex Systems (LabEx CSC, ANR-10-LABX-0026_CSC) through the post-doctoral grant of A.D. This work was supported by the International Center for Frontier Research in Chemistry (icFRC, Strasbourg) through the PhD grant of T.K. A.D. is thankfull to Prof. Coen de Graaf and Prof. Ria Broer for very valuable discussions and insights on the $LaMnO_3$ system.

References

1 M. H. V. Huynh and T. J. Meyer, *Chemical Reviews*, 2007, **107**, 5004–5064
2 R. E. Blankenship and W. W. Parson, *Annual Review of Biochemistry*, 1978, **47**, 635–653
3 T. Ameri, G. Dennler, C. Lungenschmied and C. J. Brabec, *Energy Environ. Sci.*, 2009, **2**, 347–363
4 F. Lachaud, C. Jeandon, M. Beley, R. Ruppert, P. C. Gros, A. Monari and X. Assfeld, *The Journal of Physical Chemistry A*, 2012, **116**, 10736–10744
5 M. Reyes-Reyes, K. Kim and D. L. Carroll, *Appl. Phys. Lett.*, 2005, **87**, 083506–083508
6 A. Heckmann and C. Lambert, *Angewandte Chemie International Edition*, 2012, **51**, 326–392

Dalton Transactions Accepted Manuscript

This journal is © The Royal Society of Chemistry [year]

7 C. J. Brabec, S. Gowrisanker, J. J. M. Halls, D. Laird, S. Jia and S. P. Williams, *Advanced Materials*, 2010, **22**, 3839–3856

8 S. Nishida, Y. Morita, K. Fukui, K. Sato, D. Shiomi, T. Takui and K. Nakasuji, *Angewandte Chemie International Edition*, 2005, **44**, 7277–7280

9 C. Zener, *Physical Review*, 1951, **82**, 403–405

10 R. von Helmolt, J. Wecker, B. Holzapfel, L. Schultz and K. Samwer, *Physical Review Letters*, 1993, **71**, 2331–2333

11 M. B. Salamon and M. Jaime, *Reviews of Modern Physics*, 2001, **73**, 583–628

12 J. Rodríguez-Carvajal, M. Hennion, F. Moussa, A. H. Moudden, L. Pinsard and A. Revcolevschi, *Physical Review B*, 1998, **57**, R3189–R3192

13 L. González, D. Escudero and L. Serrano-Andrés, *ChemPhysChem*, 2012, **13**, 28–51

14 E. Runge and E. K. U. Gross, *Physical Review Letters*, 1984, **52**, 997–1000

15 M. Marques, C. Ullrich, F. Nogueira, A. Rubio, K. Burke and E. Gross, *Time-Dependent Density Functional Theory*, Springer-Verlag, New York, 2006, vol. 706

16 M. E. Casida, *Journal of Molecular Structure: THEOCHEM*, 2009, **914**, 3–18

17 C. Faber, I. Duchemin, T. Deutsch and X. Blase, *Physical Review B*, 2012, **86**, 155315

18 A. J. Cohen, P. Mori-Sánchez and W. Yang, *Science*, 2008, **321**, 792–794

19 Q. Wu and T. Van Voorhis, *Physical Review A*, 2005, **72**, 024502

20 Q. Wu and T. Van Voorhis, *Journal of Chemical Theory and Computation*, 2006, **2**, 765–774

21 B. Kaduk, T. Kowalczyk and T. Van Voorhis, *Chemical Reviews*, 2012, **112**, 321–370

22 A. Domingo, M. À. Carvajal, C. d. Graaf, K. Sivalingam, F. Neese and C. Angeli, *Theoretical Chemistry Accounts*, 2012, **131**, 1–13

23 Y. Morita, T. Ohba, N. Haneda, S. Maki, J. Kawai, K. Hatanaka, K. Sato, D. Shiomi, T. Takui and K. Nakasuji, *Journal of the American Chemical Society*, 2000, **122**, 4825–4826

24 V. Barone and M. Cossi, *The Journal of Physical Chemistry A*, 1998, **102**, 1995–2001

25 M. Cossi, N. Rega, G. Scalmani and V. Barone, *The Journal of Chemical Physics*, 2001, **114**, 5691–5701

26 M.-B. Lepetit, N. Suaud, A. Gelle and V. Robert, *The Journal of Chemical Physics*, 2003, **118**, 3966–3973

27 Z. Barandiarán and L. Seijo, *Journal of Chemical Physics*, 1988, **89**, 5739–5746

28 S. E. Derenzo, M. K. Klintenberg and M. J. Weber, *Journal of Chemical Physics*, 2000, **112**, 2074–2081

29 L. Hozoi, A. H. de Vries and R. Broer, *Physical Review B*, 2001, **64**, 165104

30 C. de Graaf, C. Sousa and R. Broer, *Physical Review B*, 2004, **70**, 235104

31 A. Stoyanova, C. Sousa, C. de Graaf and R. Broer, *International Journal of Quantum Chemistry*, 2006, **106**, 2444–2457

32 A. Sadoc, R. Broer and C. de Graaf, *Journal of Chemical Physics*, 2007, **126**, 134709

33 C. de Graaf, W. A. de Jong, R. Broer and W. C. Nieuwpoort, *Chemical Physics*, 1998, **237**, 59–65

34 C. de Graaf and R. Broer, *Physical Review B*, 2000, **62**, 702–709

35 F. Aquilante, L. De Vico, N. Ferré, G. Ghigo, P.-å. Malmqvist, P. Neogrády, T. B. Pedersen, M. Pitoňák, M. Reiher, B. O. Roos, L. Serrano-Andrés, M. Urban, V. Veryazov and R. Lindh, *Journal of Computational Chemistry*, 2010, **31**, 224–247

36 B. O. Roos, R. Lindh, P.-Å. Malmqvist, V. Veryazov and P.-O. Widmark, *The Journal of Physical Chemistry A*, 2004, **108**, 2851–2858

37 B. O. Roos, R. Lindh, P.-Å. Malmqvist, V. Veryazov and P.-O. Widmark, *The Journal of Physical Chemistry A*, 2005, **109**, 6575–6579

38 M. Kepenekian, V. Robert, B. Le Guennic and C. De Graaf, *Journal of Computational Chemistry*, 2009, **30**, 2327–2333

39 B. O. Roos, P. R. Taylor and P. E. M. Siegbahn, *Chemical Physics*, 1980, **48**, 157–173

40 P.-Å. Malmqvist, A. Rendell and B. O. Roos, *Journal of Physical Chemistry*, 1990, **94**, 5477–5482

41 P.-Å. Malmqvist and B. O. Roos, *Chemical Physics Letters*, 1989, **155**, 189–194

42 K. Andersson, P.-Å. Malmqvist and B. O. Roos, *The Journal of Chemical Physics*, 1992, **96**, 1218–1226

43 N. Forsberg and P.-Å. Malmqvist, *Chemical Physics Letters*, 1997, **274**, 196–204

44 M. W. Kim, P. Murugavel, S. Parashar, J. S. Lee and T. W. Noh, *New Journal of Physics*, 2004, **6**, 156–168

45 N. N. Kovaleva, A. V. Boris, C. Bernhard, A. Kulakov, A. Pimenov, A. M. Balbashov, G. Khaliullin and B. Keimer, *Physical Review Letters*, 2004, **93**, 147204

46 A. S. Moskvin, *Physical Review B*, 2002, **65**, 205113

47 A. S. Moskvin, A. A. Makhnev, L. V. Nomerovannaya, N. N. Loshkareva and A. M. Balbashov, *Physical Review B*, 2010, **82**, 035106

48 A. Domingo, *Ph.D Thesis*, Universitat Rovira i Virgili, Tarragona, Spain, 2011

Dalton Transactions Accepted Manuscript

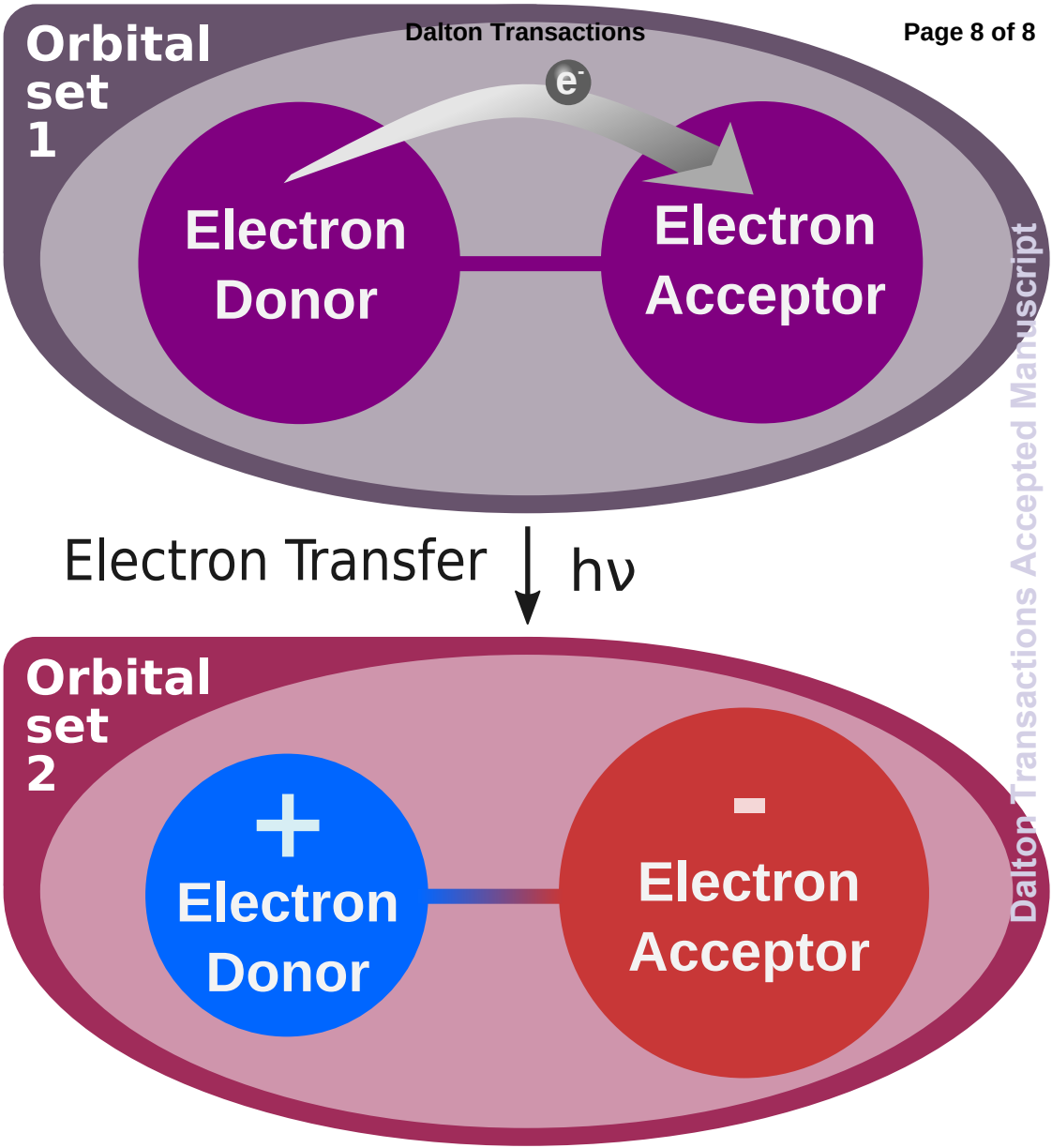

Dalton Transactions Accepted Manuscript